

STABILITY OF UNDERWATER STRUCTURE UNDER WAVE ATTACK

C. Paotonan

Engineering Faculty, Hasanuddin University, Makassar, INDONESIA
E-mail: patotonan_ch@yahoo.com

D. B. P. Allo

Civil Engineering Department, Cenderawasih University, Jayapura, INDONESIA
E-mail: daniel_bpa@yahoo.com

ABSTRACT

Geotube is, among others, a type of coastal structure that is increasingly accepted for coastal protection especially underwater breakwater. Besides its relatively low cost, it has other advantages such as flexibility, ease of construction and the fact that it can be filled with local sand material. Similar to all other coastal structures, it should also be stable under wave attack. A simple theoretical approach based on linear wave was adopted to estimate the stability of such structure. The theoretical solution was then compared with an experimental study. The experimental study was conducted at the Hydraulics and Hydrology Laboratory of Universitas Gadjah Mada. However, instead of a real geotube, PVC pipe was used where the weight of the PVC was varied by adjusting the volume of sand in the pipe. The result indicated that the agreement between the theoretical solution and the experiment was encouraging. The analytical solution may be utilized to predict underwater pipe stability under wave attack with certain degree of accuracy.

Keywords: Geotube, initial movement, submerged structure.

INTRODUCTION

Geotube is a type of coastal structure which can be used as coastal protection. Basically geotube is a geosynthetic type of material which is stitched to form a tube when filled with sand or cement material.

Geotube can be used as groin, jetty, or even breakwater as long as the material is strong enough against debris or sunlight. The advantage of geotube is its flexibility size as normally the size of geotextile is almost unlimited when stitched to one another. It is also lightweight which makes transportation easy. There are other economic advantages that make the structure increasingly acceptable.

When used as a breakwater it has to be strong enough to withstand wave force and current (Pilarczyk, 1998, 2000). For this reason, the paper discusses the stability of geotube underwater breakwater.

Researches related to geotube as a coastal structure have been carried out by many such as Shin E.C, and Oh Y.I. (2007) who studied the stability of Geotube based on two-dimensional physical model. Paotonan et al (2011) analyzed the geotube stability under sinusoidal wave attack.

The use of geotube as coastal protection has been realized in many parts of Indonesia and other countries. El Dorado Royale Resor, Mexico is one of the examples.

Geotube can also be found in Yucatan coast, Mexico to protect the eroded beach. The geotube in El Dorado Royale Resort, Mexico is a typical detached breakwater. The length of the coastal line protected by the structure is 4 km. In Indonesia, geotubes were installed in many locations, for example at Lombang coast of Tirtamaya resort area near Indramayu, West Java. The cross section of geotube may be shaped as required, though it is mostly rounded when fully filled with sand. On the other hand, the shape of the geotube will be close to ellipse when the sand fill is not full. In this paper, the geotube was assumed to be fully filled with sand and the shape was nearly round.

THEORETICAL APPROACH

The forces acting on a geotube are drag force, inertia force, lift force, gravitational force, buoyancy force that is described below.

A. Gravitational force

The weight of the structure in air (W_a) may be written as:

$$W_a = \rho_s g V_s \quad (1)$$

Where ρ_s is geotube specific mass, V_s is volume per meter length of geotube, and g is earth gravitational acceleration. The unit of ρ_s , V_s , and g are kg/m^3 , m^3/m , and m/s^2 respectively. If the cross section is round with diameter D in meter, the weight of geotube is

$$W_a = \rho_s g \pi \frac{D^2}{4} \quad (2)$$

The buoyancy force (F_B) that is responsible for the reduced weight in the water can be written as:

$$F_B = \rho g V_s \quad (3)$$

alternatively, for cylindrical geotube it reads

$$F_B = \rho g \pi \frac{D^2}{4} \quad (4)$$

The net force on geotube in the water is given by Equation 5.

$$W_R = (\rho_s - \rho) g \pi \frac{D^2}{4} \quad (5)$$

B. Lift Force

When wave propagates above the geotube, there should be different velocities from the top to the bottom of the geotube. In fact, the velocity at the bottom of geotube may be regarded as zero or no flow. The flow above the geotube may be assumed to follow the linear wave theory (Figure 1). Due to such differential flow, there is vertical force (lift force) acting on the geotube.

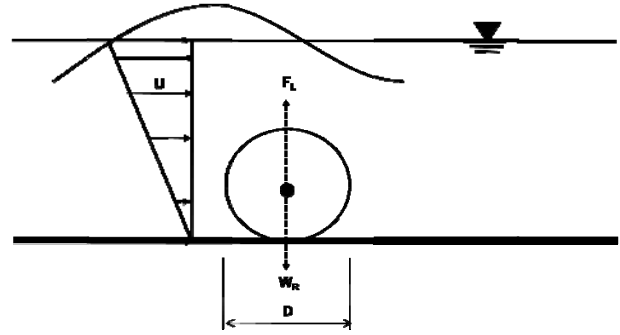


Figure 1. Lift force on the geotube

The lift force was given by Dean (1992) as in this equation

$$F_L = C_L \rho \frac{D}{2} u^2 \quad (6)$$

Where u is velocity at the top of the structure in m/s , and C_L is a lift force coefficient. Lift force coefficient on cylindrical body is 4.493 (Wilson and Reid 1963). In shallow water, velocity under linear wave is simply

$$u = a \sqrt{\frac{g}{h_s}} \quad (7)$$

Where h_s is the depth at the toe of the geotube and a is wave amplitude.

Substituting u in Equation 7, using Equation 8 yields

$$F_L = \frac{C_L}{2} \rho g a^2 D / h_s \quad (8)$$

or

$$F_L = C_L \rho g \frac{H^2}{8} D / h_s \quad (9)$$

where H is wave high.

C. Drag force

The drag force takes the form of

$$F_D = C_D \rho \frac{D}{2} u^2 \quad (10)$$

Where C_D is drag force coefficient, which varies from 1 to approximately 2.2 and is a function of Keulegan Carpenter (Dean and Dalrymple, 1986). Equation 10, drag force is function of velocity and geotube diameter.

For the case of submerged geotube, velocity distribution can be simplified and drawn as in Figure 2.

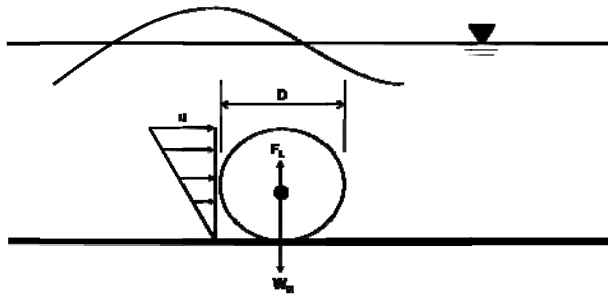


Figure 2. Simplification of velocity distribution on submerged geotube

On Figure 2, distribution of velocity in triangular. For simplification, average velocity is considered. Therefore, structure is located in shallow water then equation 10 can be written as:

$$F_D = \frac{C_D}{2} \rho g a^2 D / h_s \quad (11)$$

Or

$$F_D = C_D \rho g \frac{H^2}{8} D / h_s \quad (12)$$

D. Geotube initial motion

When an object (geotube) is submerged in the water, there are two possible modes of initial motion. The first is due to vertical force as described by Equation 13.

$$W_R = (\rho_s - \rho) g \pi \frac{D^2}{4} - C_L \rho g \frac{H^2}{8} D / h_s \quad (13)$$

In this case, the geotube is not stable when the total force due to buoyancy and lift force is larger than the weight of the structure. The second mode is due to the combined forces of vertical and horizontal forces (drag force) as given by Equation 14.

$$f \left((\rho_s - \rho) g \pi \frac{D^2}{4} - C_L \rho g \frac{H^2}{8} D / h_s \right) \quad (14)$$

$$= C_D \rho g \frac{H^2}{8} D / h_s$$

The coefficient f is introduced in Equation 14 as the friction factor between the geotube and the bottom. The friction coefficient f ranges from as little as 0.0002 (on steel) to as high as 0.4 (loose sand). In this experiment, the model was placed at the bottom of the flume, which was slightly corroded steel. Therefore, in this matter the value of f will be varied to find out the correlation between the experimental data and the theoretical result. Equation 14, can be simplified as:

$$f \left(\frac{\rho_s}{\rho} - 1 \right) \pi D - f C_L \frac{H^2}{2} / h_s = C_D \frac{H^2}{2} / h_s \quad (15)$$

or

$$f \left(\frac{\rho_s - \rho}{\rho} \right) \pi D = \frac{f C_L + C_D}{2} H^2 / h_s \quad (16)$$

Since the drag force coincides with the lift force, the second mode is more likely to occur. The wave height required to destabilize the geotube may be written as:

$$H = \sqrt{\frac{2f \left(\left(\frac{\rho_s}{\rho} - 1 \right) \pi D \right) h_s}{f C_L + C_D}} \quad (17)$$

In non-dimensional parameter form, Equation 15 can be written as:

$$\frac{H}{D} = \sqrt{\frac{2f \left(\left(\frac{\rho_s}{\rho} - 1 \right) \pi \right) h_s}{f C_L + C_D} \frac{1}{D}} \quad (18)$$

Therefore, the non-dimensional parameters relevant to the initial motion of the geotube are H/D , $\frac{\rho_s}{\rho} - 1$ and $\frac{h_s}{D}$. Equation 16 will be used to calculate minimum wave height needed for the structure to start moving.

E. Physical Model Simulation

The experimental study was conducted in a regular wave flume of 30 cm wide. PVC pipes of different sizes that were closed at both ends were used as geotube models. In order to vary the weight of the model and hence its overall density, the pipes were filled with water and sand of different volumes. The diameter of the pipes was 13.02 cm (model I), 11.02 cm (model II) and 8.374 cm (Model III). The models are shown in Figure 3.

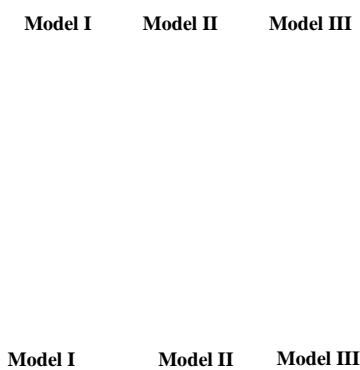


Figure 3. Model of geotubes

Each model was tested under sinusoidal waves attack. The test was initiated using small wave amplitudes and was increased at small increment to observe the initial motion of the geotube models that indicate instability. The wave heights were measured using wave probes. The geotube model during the test is shown in Figure 4.

Model

Figure 4. Testing models in the wave flume

The models were run for all (three geotubes) models. The results, together with the analytical approach, were given in the next section.

RESULTS AND DISCUSSION

The results of the experimental work are given in Table 1 and Figure 5. It can be seen that the agreement between the theoretical and the experimental data is encouraging. However, the real friction coefficient has to be determined for better comparison. In this study, the friction coefficients was tried and the best fit was chosen. Hence, with such value of f (the best fit) only a trend comparison between the experiment and the theoretical solution can be made. The final trial indicated that $f = 0.00546$ produced the best fit.

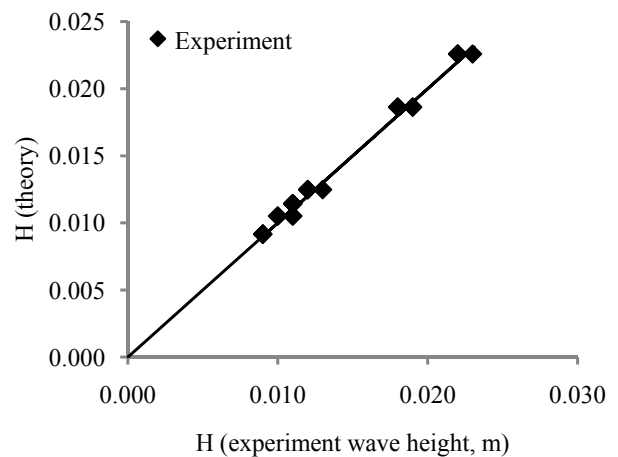


Figure 5. Theoretical vs Experimental wave height required for geotube models initial motion ($f = 0.00546$; $C_D = 2.200$ and $C_L = 4.489$)

Table 1. Experimental and theoretical minimum wave height for geotubes model stabilization

| Model Specification | m (kg) | V (m^3) | ρ_s (kg/m^3) | D (m) | h_s (m) | H (experiment, m) | H (theoretical, m) with $f = 0.00546$ (-) |
|-----------------------|-------------|------------------|--------------------------|------------|--------------|------------------------|--|
| I 100% of water | 4.516 | 0.004 | 1.2600 | 0.130 | 0.250 | 0.0110 | 0.0110 |
| | 4.516 | 0.004 | 1.2600 | 0.130 | 0.250 | 0.0110 | 0.0110 |
| | 4.516 | 0.004 | 1.2600 | 0.130 | 0.250 | 0.0110 | 0.0110 |
| | 4.516 | 0.004 | 1.2600 | 0.130 | 0.250 | 0.0110 | 0.0110 |
| | 2.965 | 0.003 | 1.2600 | 0.110 | 0.250 | 0.0110 | 0.0110 |
| | 2.965 | 0.003 | 1.2600 | 0.110 | 0.250 | 0.0110 | 0.0110 |
| | 2.965 | 0.003 | 1.2600 | 0.110 | 0.250 | 0.0100 | 0.0110 |
| | 2.965 | 0.003 | 1.2600 | 0.110 | 0.250 | 0.0100 | 0.0110 |
| | 3.481 | 0.003 | 1.3660 | 0.110 | 0.250 | 0.0130 | 0.0120 |
| | 3.481 | 0.003 | 1.3660 | 0.110 | 0.250 | 0.0120 | 0.0120 |
| | 3.481 | 0.003 | 1.3660 | 0.110 | 0.250 | 0.0120 | 0.0120 |
| | 3.481 | 0.003 | 1.3660 | 0.110 | 0.250 | 0.0120 | 0.0120 |
| II 75% of dry sand | 4.627 | 0.003 | 1.8170 | 0.110 | 0.250 | 0.0180 | 0.0190 |
| | 4.627 | 0.003 | 1.8170 | 0.110 | 0.250 | 0.0190 | 0.0190 |
| | 4.627 | 0.003 | 1.8170 | 0.110 | 0.250 | 0.0180 | 0.0190 |
| | 4.627 | 0.003 | 1.8170 | 0.110 | 0.250 | 0.0190 | 0.0190 |
| | 5.605 | 0.003 | 2.2000 | 0.110 | 0.250 | 0.0220 | 0.0230 |
| | 5.605 | 0.003 | 2.2000 | 0.110 | 0.250 | 0.0220 | 0.0230 |
| | 5.605 | 0.003 | 2.2000 | 0.110 | 0.250 | 0.0220 | 0.0230 |
| | 5.605 | 0.003 | 2.2000 | 0.110 | 0.250 | 0.0230 | 0.0230 |
| | 1.845 | 0.001 | 1.2600 | 0.0840 | 0.250 | 0.0090 | 0.0090 |
| | 1.845 | 0.001 | 1.2600 | 0.0840 | 0.250 | 0.0090 | 0.0090 |
| | 1.845 | 0.001 | 1.2600 | 0.0840 | 0.250 | 0.0090 | 0.0090 |
| | 1.845 | 0.001 | 1.2600 | 0.0840 | 0.250 | 0.0090 | 0.0090 |
| III 100% of water | 1.845 | 0.001 | 1.2600 | 0.0840 | 0.250 | 0.0090 | 0.0090 |
| | 1.845 | 0.001 | 1.2600 | 0.0840 | 0.250 | 0.0090 | 0.0090 |
| | 1.845 | 0.001 | 1.2600 | 0.0840 | 0.250 | 0.0090 | 0.0090 |
| | 1.845 | 0.001 | 1.2600 | 0.0840 | 0.250 | 0.0090 | 0.0090 |

Figure 5 shows that the trend of the experimental wave heights that agree with the theoretical solution. Using regression technique a fitting curve as in Figure 5 indicates a slope of unity, showing the best fit of the f value and indicates the agreement of the experimental and theoretical data trend. The parameter for the best agreement was 0.00546; 2.200, and 4.493 for f , C_D , and C_L respectively at the initial movement of a submerged coastal structure. In terms of non dimensional parameter, the results of the experiment may be compared with the theoretical solution in Figure 6 and Figure 7.

Figure 6 shows that increasing value of $(\rho_s/\rho-1)$ causes the increasing value of H/D , which means that when the value of specific gravity of structure increases, the wave height required to stir the structure is greater. If the geotube specific gravity and the water depth are constant, the

effect of water depth and geotube diameter ratio on H/D can be obtained. The influence of h_s/D on H/D for a constant ρ_s/ρ can be seen in Figure 7.

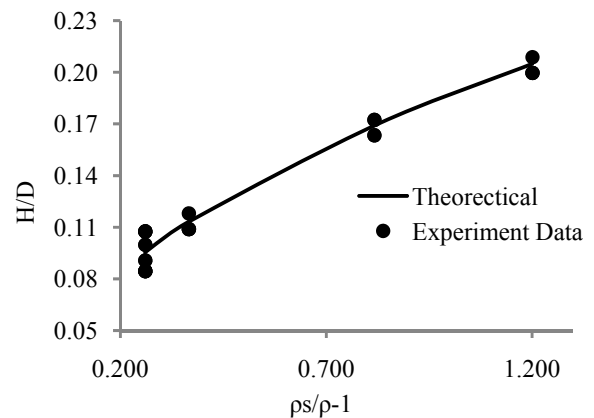


Figure 6. Relationship between $\rho_s/\rho-1$ and H/D

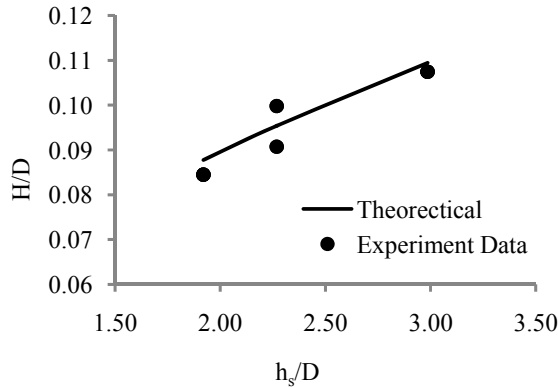


Figure 7. Relationship between h_s/D and H/D

Again, Figure 7 shows that the trend between the measurements in the laboratory and the theoretical calculation is similar. The increasing value of h_s/D causes the increasing H/D value. Using Equation 16 the combination of non dimensional parameter that affects H/D is $\left(\frac{\rho_s}{\rho} - 1\right) \frac{h_s}{D}$ where the correlation is indicated in

Figure 8. The line and scatter point in the Figure are theoretical line and data experiment, respectively.

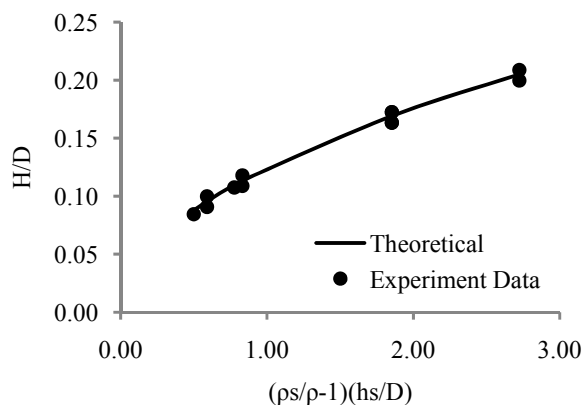


Figure 8. The combinative effects of $\rho_s/\rho - 1$ and h_s/D on H/D

Figure 8 shows the increasing value of $(\rho_s/\rho - 1)(h_s/D)$ causes the increasing values of H/D . Theoretical value of H/D on Figures 5 to 8, were calculated by assuming that f , C_D , and C_L values were 0.00546; 2.200 and 4.498 respectively. Using Equation 17, H/D values as a function of geotube specific gravity and ratio of depth water to geotube diameter can be calculated where the result is presented in Figure 9.

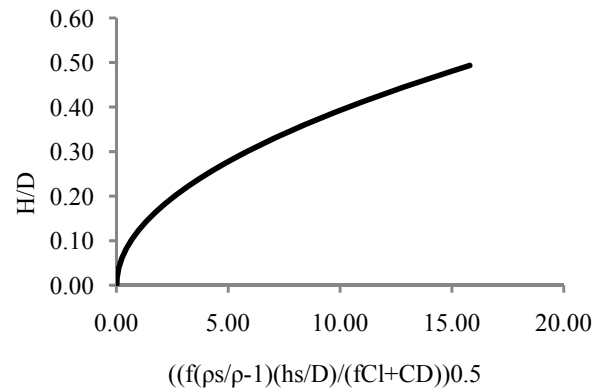


Figure 9. Geotube Initial movement graph

Using Figure 9, the initial movement of submerged structure can be predicted. A situation that is represented by a point located above of the curve of Figure 9 is unstable and vice versa. Suppose a geotube under wave attack of $(\rho_s/\rho - 1)(h_s/D) = 5.0$ and $H/D = 0.4$ it indicates that the structure is theoretically unstable while a geotube of $(\rho_s/\rho - 1)(h_s/D) = 5.0$ and $H/D = 0.1$ is theoretically settled.

CONCLUSIONS

Based on the explanation above, it can be concluded into some points below. Firstly, the stability of a submerged structure is influenced by wave parameters (height and water depth) and structure parameters; those are the specific gravity and the diameter of structure, D . Secondly, the wave height trend which is able to move the structure obtained from experimental data and calculation with Equation 15 are equal. Thirdly, as the value of structure specific gravity increases, the wave height which is needed to move the structure is increasing too. Or in other words as the specific gravity of structure increases, the structure is more stable as well. Fourthly, if the value of water depth and structure diameter is getting greater, the effect on wave height and structure diameter ratio is getting greater and follows the logarithmic trend. Combination of non-dimensional parameter which influences the ratio of wave height value and structure diameter is $(\rho_s/\rho - 1)(h_s/D)$. As the value of $(\rho_s/\rho - 1)(h_s/D)$ increases, the value of H/D increases too. The initial movement of geotube can be predicted by using Equation 17 or Figure 9.

ACKNOWLEDGMENTS

The authors would like to thank Directorate General of Higher Education (DIKTI) and Hasanuddin University for financial support to do the research. Invaluable comments, suggestions and corrections by Prof. R. Triatmadja especially with respect to the stability of geotube of the original paper is highly appreciated. The authors also express their sincere gratitude to the Head of the Centre of Engineering Science Studies and the Head of Hydraulics and Hydrology Laboratory, Universitas Gadjah Mada, for the facilities to support this research.

REFERENCES

- Dean, R.G. and Dalrymple, R.A. (1993). *Water Wave Mechanics for Engineer and Scientist*. World Scientific Publishing. Singapore.
- Koerner, G.R., Koerner, R.M. (2006). *Geotextile tube assessment using a hanging bag test*. Geotextiles and Geomembranes 24 (2), 129–137.
- Muthukumar, A.E., Ilamparuthi, K. (2006). *Laboratory studies on geotextile filters as used in geotextile tube dewatering*. Geotextiles and Geomembranes 24 (4), 210–219.
- Oh, Y.I., and Shin, E.C. (2006). *Using submerged geotextile tubes in the protection of the E. Korean shore*. Coastal Engineering 53 (2006) 879–895, accepted 1 June 2006, www.Sciencedirect.com.
- Paotonan, C, Nur Yuwono, Radiana Triatmadja, and Bambang Triatmodjo (2011). *Theoretical Approach of Geotextile Tube Stability as a Submerged Coastal Structure*. Proceeding of International Seminar on Water Related Risk Management, Jakarta.
- Pilarczyk, K. W. (1995). *Novel systems in coastal engineering: Geotextile systems and other methods, an overview*. HYDRO pil Report, Road and Hydraulic Engineering Division of the Rijkswaterstaat, Delft, The Netherlands.
- Pilarczyk, K.W. (1999). *Geosynhtetics and Geosystem in Hydraulic and Coastal engineering*, A. A Balkema, Rotterdam (balkema@balkema.nl; www.balkema.nl).
- Pilarczyk, K.W. (1998). *Stability criteria for geosystems—an overview*. Proceedings of the Sixth International Conference on Geosynthetics, Atlanta, USA, vol. 2. pp. 1165–1172.
- Pilarczyk, K.W. (2000). *Geosynthetics and Geosystems in Hydraulic and Coastal Engineering*. A.A. Balkema, Rotterdam.
- Shin E.C. and Oh Y.I. (2007). *Coastal erosion prevention by geotextile tube technology*. Geotextiles and Geomembranes 25 (2007) 264-277.
- Sprague, C.J. (1995). *P.E.T. Geotextile tube and containers for beneficial use of dredged material*. Contract Report for Bradley Industrial Textiles, Inc., Valparaiso, FL, and Hoechst Celanese Corporation, Spunbond Business Group, Spatan.

[this page intentionally left blank]